Nonlinear and Chaotic Circuits

Adrian Thompson

Physics 134 Advanced Laboratory
Lab Partner: Alex Barker
University of California, Santa Cruz

June 8, 2014

Abstract

We studied the behavior of nonlinear and chaotic circuits. The resonant frequency of an LRC circuit was experimentally determined, and the circuit was compared to a diode-inductor-resistor (DLR) circuit to explore the transition from nonlinearity to chaos. The internal resistance of the LRC inductor was found to be $123 \pm 2\ \Omega$, while the low amplitude diode capacitance of the DLR circuit was found to be 55.6 ± 0.7 pF. With the aid of a fast-Fourier-transform (FFT) oscilloscope function, four regimes of behavior in the DLR circuit were studied. Finally, an experiment on Chua's strange attractor circuit is proposed as a future project.

1 Introduction

The idea of chaos as a mathematical construct, rather than as a poetic or political notion of unpredictability and noise, arose in tandem with the birth of physical dynamics. Dynamics, of course, began with Newton and his contemporaries. In that time, many problems like the many-body problem posed difficulties, in that they were impossible to solve exactly. The universal goal of every dynamics problem was to obtain the equations of motion explicitly, but for many systems, this could not be done. These systems were often described by nonlinear differential equations, and the tools used to deal with such systems had not been invented yet; or not known of, at the least.

It was not until the computer age that mathematicians and physicists could deeply investigate nonlinear systems. Lorenz made a great breakthrough in 1963, discovering the strange attractor; an aperiodic system that migrated unpredictably between two attracting steady states. Chaos, as a field of dynamics, was born and in full flourish. Many iconic mathematical objects and structures came out of this period, including the fractal, which is an infinitely self-similar set of points whose structure may be determined by chaotic equations. Benoit Mandelbrot, who is most known for his studies in fractals, invented the Mandelbrot set, the most easily recognizable fractal. It was not just mathematicians, but artists as well, who were captivated by the beautiful geometries of attractor "scrolls" in 3-D spaces, fractals, and bifurcation diagrams; all motivated to join the mathematical complexity of nature with the colorful vibrancy of brushwork or computer art [1]. Since its origin, chaos theory has provided not just mathematical beauty, but powerful practicality as well. Chaos continues to be applied in cryptography, random noise simulation, genetics, sociology, and even ecology.

In this experiment, we studied several of the fundamental elements of chaos, including bifurcation and period doubling, nonlinearity, and indeterminism. We focused on the transition between nonlinear and chaotic behavior.

1.1 Differentiating nonlinearity from Chaos

The following discussion is inspired by Stefano Profumo's *Mechanics* lectures on chaos in Fall 2013 at UC Santa Cruz.
It is easy to mistake a nonlinear dynamical system for a chaotic one. Therefore, when we discuss a chaotic system in the context of physics or mathematics, it is important to know the definition. A semi-formal definition is given:

Definition 1. *A system is chaotic if it meets the following requirements.*
1. Solutions to the equations of motion of the system are nonlinear, i.e. if ϕ_1 and ϕ_2 are solutions then $\phi_1 + \phi_2$ is not a solution.

2. The equations of motion written as functions of the degrees of freedom ξ_i

$$\frac{\partial \xi_i}{\partial t} = f(\xi_1, ..., \xi_N)$$

must have $N \geq 4$.

This definition is slightly over-cautious. To see why this is, we introduce two types of chaotic systems; dissipative and non-dissipative. Dissipative systems are those which have an overall decay after a characteristic time. The usual equations of motion are typically controlled by the multiplier $e^{\frac{-t}{\tau}}$. Dissipative systems only require that $N \geq 3$, unlike non-dissipative systems which require 4 degrees of freedom or greater. This is the source of the caution in Definition 1. In a sense, dissipative systems are readily made chaotic as one adds in variables or degrees of freedom, more so than non-dissipative systems.

1.2 Lyapunov Formulation

Other ways to define chaos exist. For example, here is a more qualitative definition: a chaotic system is one that has indeterministic behavior over a characteristic time scale, one that responds easily to small changes in the environment, and one that allows driving pulses to persist [2].

These statements about the sensitivity to initial conditions can be made quantitative by examining the time evolution of a chaotic system. Let there be two possible, infinitesimally close, trajectories in phase space $\vec{w}(t)$ and $\vec{u}(t)$. At $t = 0$ let there separation be the vector $\boldsymbol{\delta}(0) = \vec{w}(0) - \vec{u}(0)$. As the system time evolves, its trajectory becomes $\boldsymbol{\delta}(t)$ such that $|\boldsymbol{\delta}(t)| \sim e^{\lambda t}|\boldsymbol{\delta}(0)|$. λ is called the Lyapunov exponent, named after the Russian mathematician and physicist Aleksandr Lyapunov. λ tells interesting information about a chaotic system if it can be computed. It may tell how quickly these infinitesimally close trajectories diverge. For instance, if λ is positive, there will be a so called "time horizon," on the trajectories of the system. Before the time horizon, measurements on the initial conditions lead to good predictions of the future of the system. After the horizon, however, predictions fail. This time is given by

$$t_{\text{horizon}} \sim \mathcal{O}\left(\frac{1}{\lambda} \ln \frac{a}{|\boldsymbol{\delta}(0)|}\right)$$

where $a = \max \boldsymbol{\delta}(t)$ that one may allow [1].

It should be stressed that chaotic systems are mathematically deterministic in their entirety. In the world, they cannot possibly be seen as such because unavoidable uncertainties in the initial conditions of a system exist. Even small uncertainties, when time evolved by a chaotic Hamiltonian, can lead to many bifurcations. Mathematically, this means that after a sufficient time the space of all possible functions that satisfy the initial conditions and constraints on the problem, or the solution space, is very large, and spanned by a family of functions whose defining parameters have large uncertainty. This fact makes chaotic systems practically indeterministic.

In these experiments we studied a particular type of chaotic circuit which reduces to an LRC circuit at low driving amplitudes; it is the Diode-Inductor-Resistor (DLR) circuit shown in Figure 1.

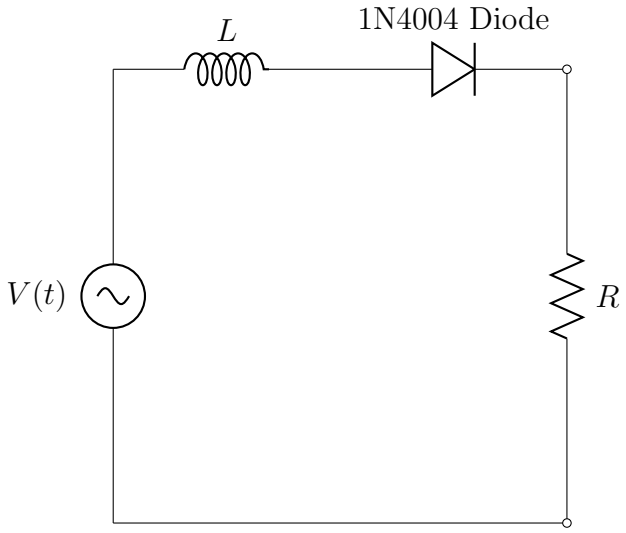

Figure 1: The DLR Circuit

In order to properly analyze the circuit, its true resistance must be known, which is not simply the resistance of R. The inductor has its own intrinsic resistance, which is non-negligible. We can represent this through a lumped circuit element diagram, as in Figure 2.

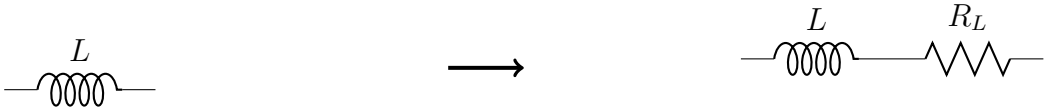

Figure 2: The lumped circuit diagram for the inductor.

We then take the total resistance in the circuit to be $R_T = R + R_L$.

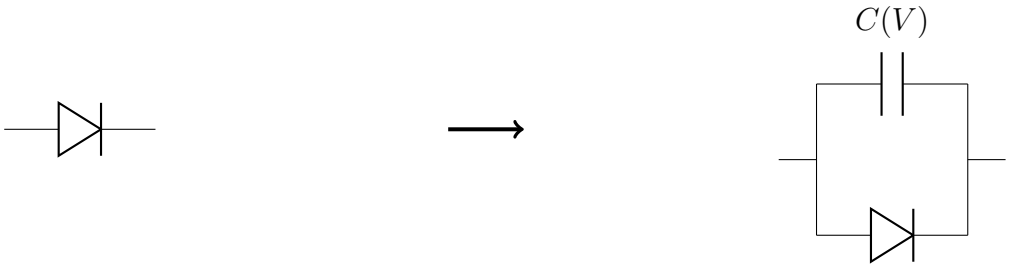

Figure 3: The lumped circuit diagram for the diode.

The diode is a nonlinear circuit element. Notice, as in Figure 3, that the diode element can be drawn as an ideal diode in parallel with a voltage dependent capacitance. This fact arises from the behavior of the p-n junction within the diode. The voltage across the diode is given by

$$V_d = \frac{kT}{e} \ln \left[1 - \frac{I}{I_r} \right]. \tag{1}$$

Here k is Boltzmann's constant, T is the temperature, e is the charge of the electron, and I_r is the reverse current in the diode junction. We then add the voltages of each component in series

and set them equal to the driving voltage;

$$V(t) = L\frac{dI}{dt} + I(R_T) + \frac{kT}{e}\ln\left[1 - \frac{I}{I_r}\right]. \tag{2}$$

This is a first order nonlinear differential equation. If we compare Equation 2 to Definition 1, we can see how the DLR circuit is a chaotic system. First, we can rewrite the diode voltage using the capacitance in parallel, with a reverse current;

$$\begin{aligned} V_d &= \frac{Q}{C(V)} \\ &= \frac{1}{C(V)}\int (I - I_r)dt \end{aligned}$$

Then, if we write $\frac{dI}{dt}$ as a function of the free variables I, V, $C(V)$, and Q, we obtain an "equation of motion" in the form of Definition 1 with $N = 4$. That, along with the clear nonlinearity in V_d, satisfies the prerequisites for chaos.

This circuit also exhibits behavior known as **bifurcation**. Bifurcation has a number of loose definitions. It is best defined as follows: Say a system has a set of control parameters $\boldsymbol{\eta} = (\eta_1, \eta_2, ..., \eta_n)$. Then, for some position in parameter space, the number of critical points in the equations of motion will change [1]. For instance, in the DLR circuit, its point of bifurcation leads to period doubling of the signal. The critical point here occurs in the phase. If the phase is ϕ, the bifurcation occurs when $\frac{\partial\phi(t,\boldsymbol{\eta})}{\partial t} = 0 \rightarrow \frac{\partial\phi(t,\boldsymbol{\eta})}{\partial t} = \text{constant}$ or $\frac{\partial\phi(t)}{\partial t} = g(t)$ where g is nonzero. So, the function $\phi(t, \boldsymbol{\eta})$ in parameter space has a critical point for some value of $\boldsymbol{\eta}$. For the DLR circuit, it will be the frequency parameter ω which, when varied, will induce a bifurcation in the form of period doubling. We observed this in the circuit and it is discussed in section 3.

2 Methods

To study our circuits, we used a *B&K Precision 3011 2MHz Function Generator* as a voltage source, and a *Tektronix TDS 2001C* oscilloscope to monitor the ingoing and outgoing signals. The two circuits that we studied were a LRC circuit and a DLR circuit. These were good circuits to study the transition from nonlinearity to chaos, because the diode, being a nonlinear circuit element, does behave like a capacitor at low driving voltages. In this way, the DLR circuit reduces to a linear, resonant circuit at low driving amplitudes. The diagrams for the two circuits are shown in Figures 5 and 6. In each, we measured the voltage across the resistor using the oscilloscope. The function generator and oscilloscope inputs all shared a common ground, and we displayed the direct driving signal from the function generator on channel 1 (CH1) of the oscilloscope. The signal across the resistors was displayed on channel 2 (CH2).

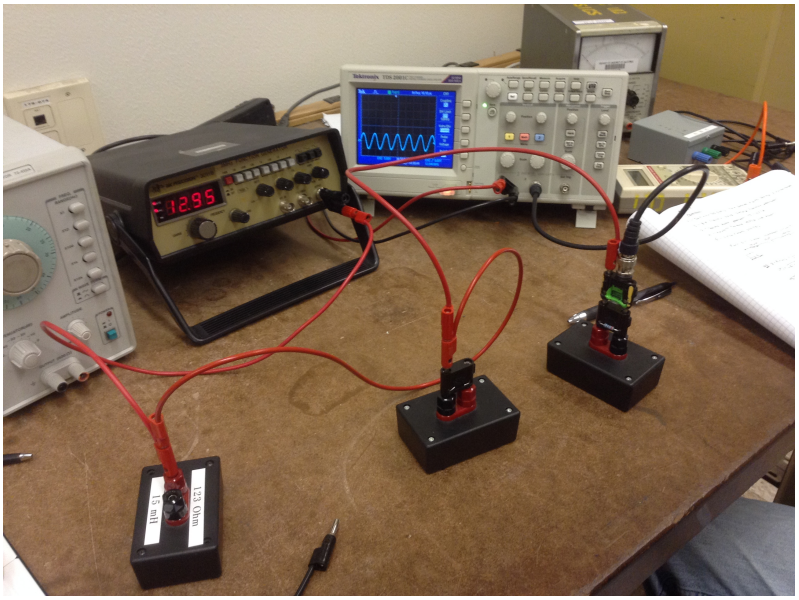

Figure 4: Our workstation, set up to take data on our constructed LRC circuit. The inductor (left), capacitor (middle) and resistor (right) are shown, contained in their black boxes.

2.1 Two Circuits

We first examined the LRC circuit. Since we knew the component values a priori as shown in Figure 5, we used equation 3 to estimate the resonance frequency of the circuit. Recall the condition for resonance frequency;

$$\omega_0^2 = \frac{1}{LC}. \tag{3}$$

$$\frac{1}{LC} = \frac{1}{15\text{mH} \cdot 10\text{nF}}$$

$$\rightarrow \omega_0 = 8.165 \cdot 10^4 \frac{\text{rad}}{\text{s}}$$

$$\rightarrow f_0 = 1.3 \cdot 10^4 \text{Hz}$$

or $f_0 = 13$ kHz.

The phase on resonance is given by the following equation.

$$\tan(u) = \frac{\omega^2 - \omega_0^2}{\omega\Gamma} \tag{4}$$

$$\Gamma = \frac{R_T}{L}$$

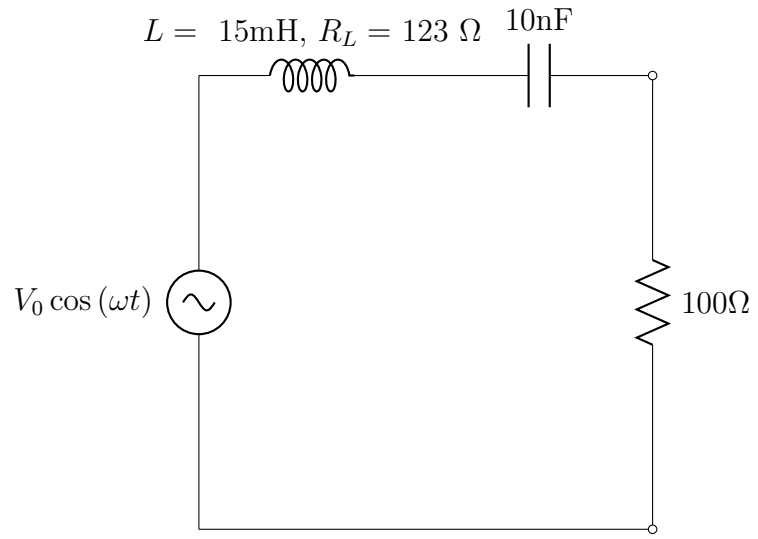

Figure 5: The Resonant LRC Circuit

We then examined the DLR circuit. To experiment on its linearity at low amplitudes, we activated the attenuator on the BK function generator by pulling out the amplitude knob. This drove the circuit at input voltages in the range of 500mV to 1V.

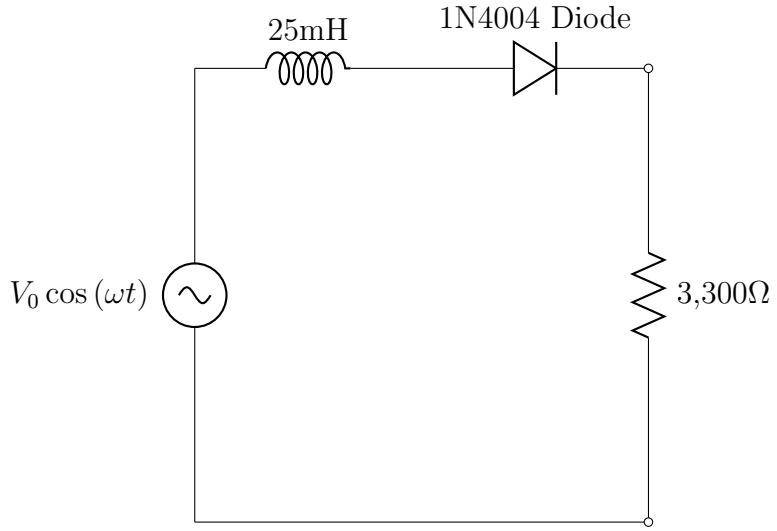

Figure 6: The DLR Circuit

Just as before, we took voltage and frequency data in order to plot the frequency response of the circuit. This allowed us to find the resonance frequency, which at low amplitudes, is a good first order approximation to the LRC resonance frequency;

$$\omega_0^2 = \frac{1}{LC}. \tag{5}$$

We then used the known value of the inductance (25 mH) and the found resonance frequency to calculate the capacitance of the diode junction described in Figure 3. With the attenuator activated, the amplitudes should be low enough such that $C(V)$ is homogeneous, or stable in that range of input voltages.

2.2 Regimes of Nonlinearity and Chaos

We wanted to see how the circuit behaved at higher amplitudes. We made use of the fast-fourier-transform (FFT) function on the oscilloscope. It was displayed by using "Math" → "FFT". This

was a great feature which used an internal chipset to perform fast integrations in order to display the frequency spectrum of a signal on the screen. This allowed us to see distinct amplitude regimes which were uniquely characterized by different frequency spectrums. These are shown in the following section.

Another feature is the XY display function on the oscilloscope, which we used to view the periodicity or aperiodicity of the circuit, and to easily view the relationship between the current and voltage in the circuit. This is essentially an IV (current-voltage) curve, with one caveat; it's really a voltage-voltage curve that plots the CH1 voltage on one axis and the CH2 voltage on the other. Since the phase difference is equivalent to the phase between the current in the circuit and the voltage we measured on CH2, we referred to it as an IV curve. The key here was not to pay too much attention to the relative amplitudes, rather, to look at the phase.

3 Results

3.1 The Resonant Circuit

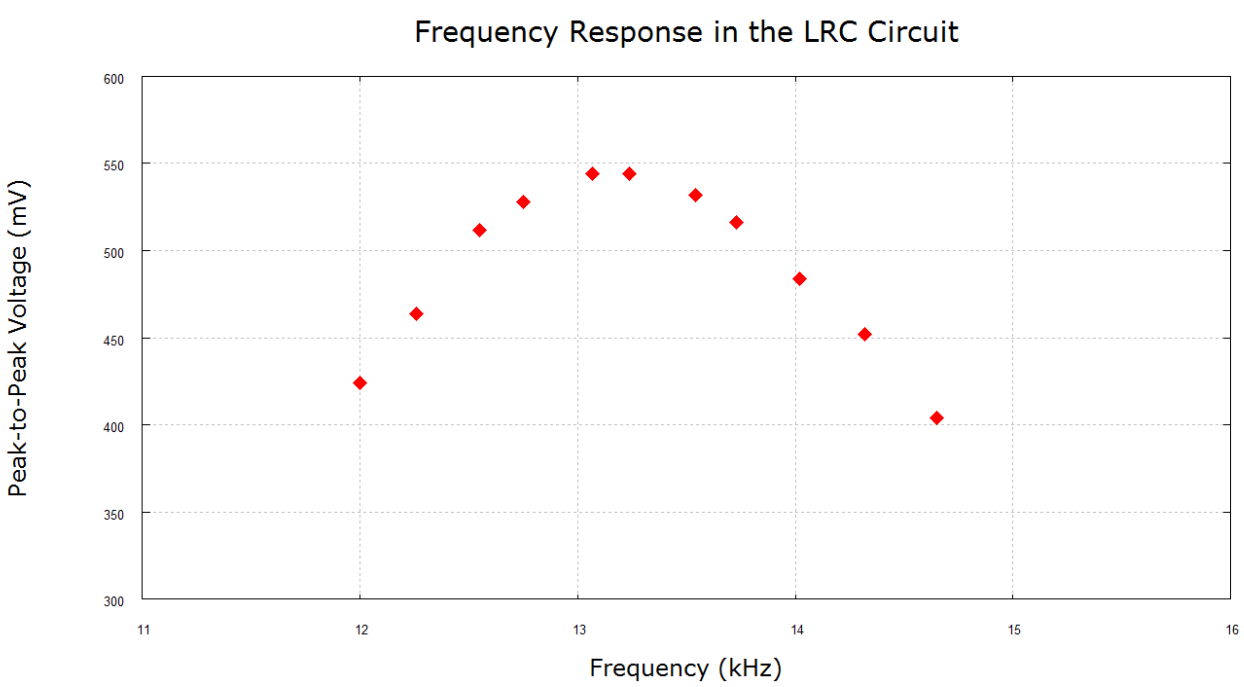

Figure 7

Figure 7 shows the frequency response of the LRC circuit about the predicted resonance frequency. We also plotted the tangent of the phase as a function of frequency, as in equation (4). Since we took data in Hertz, we changed the equation to be a function of pure cycles per second. Also, a sign change had to be made to account for the measured phase to be of opposite sign.

$$\tan(u) = 2\pi \frac{f_0^2 - f^2}{f \cdot \Gamma}$$

Figure 8 shows the fit.

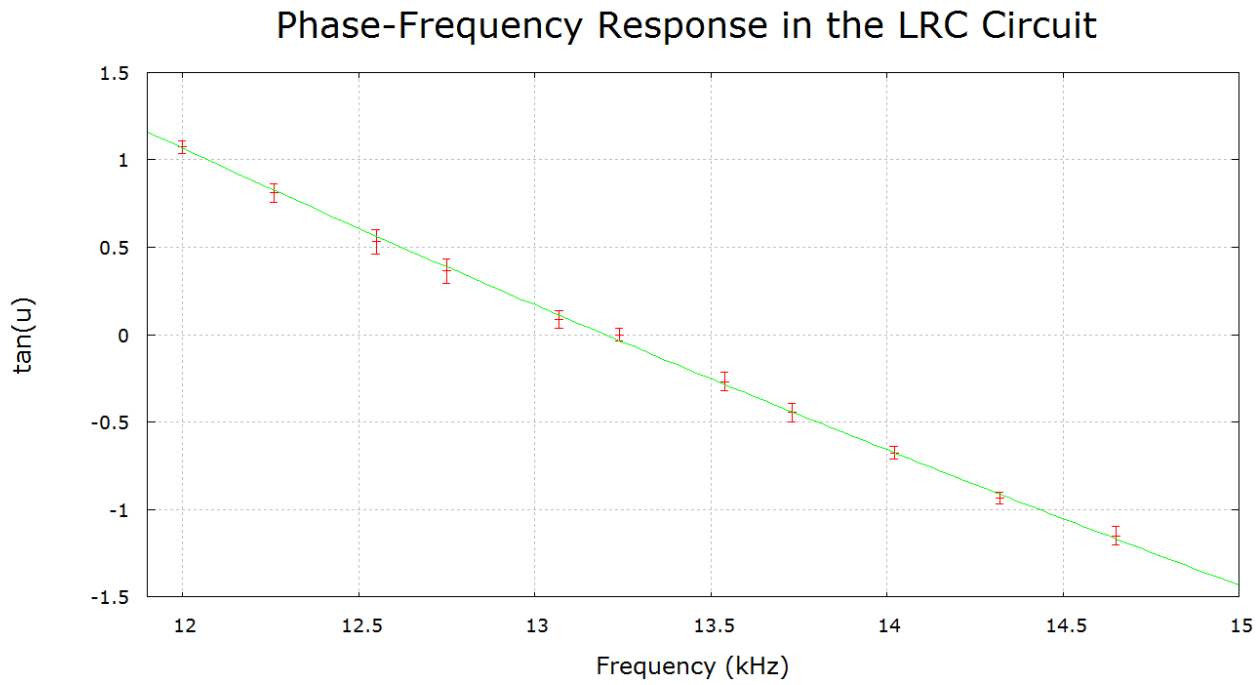

Figure 8: Here the phase difference between current and voltage is denoted u. The tangent of the phase is plotted against frequency; note that resonance is achieved at $u = \tan(u) = 0$, at 13.20 kHz.

From the Gnuplot fit, we extracted the resonant frequency f_0 and Γ, from which we obtained the intrinsic resistance of the inductor, R_L. The results are shown below.

LRC Results

$$f_0 = 13.20 \pm 0.01 \text{ kHz}$$
$$\Gamma = 14839.2 \pm 135.3 \text{ s}^{-1}$$
$$R_L = 123 \pm 2 \ \Omega$$

This matched up well with the prediction we made in section 2.2 of $f_0 = 13$ kHz. It especially matched well with the claimed resistance of the inductor of 123 Ω, as in Figure 5.

3.2 The DLR Circuit

We began by spanning a range of frequencies at an attenuated amplitude on the diode circuit. We found a resonance at around 130 kHz, so we performed a frequency sweep about that resonance and took voltage and phase data. Figure 9 shows the frequency response and the peak resonance.

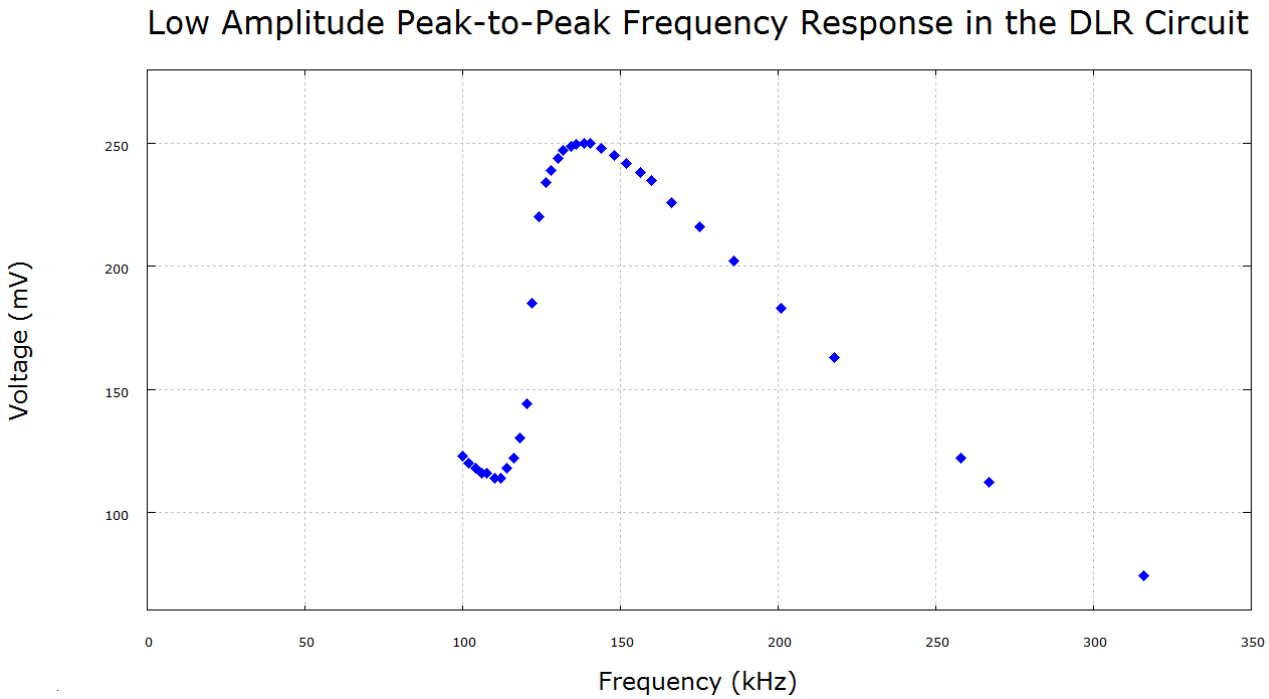

Figure 9

We performed the same fit as before on the DLR circuit data. Gnuplot's fit gave us a value for the resonant frequency, which we then used to calculate the diode capacitance. Here we had to be careful; since the frequency response of the DLR circuit was behaving strangely at lower frequencies (i.e. the rising low end tail in Figure 9), we took this to be irreducible nonlinear behavior. So, we only performed a fit to the middle region of the graph which was most symmetric. We used the known value of L for this calculation (see Figure 6). We obtained the error on C by performing some error propagation;

$$C = \frac{1}{4 * \pi^2 f_0^2 L}$$
$$\sigma_C^2 = \frac{1}{4\pi^4 L^2 f_0^6} \sigma_{f_0}^2 \tag{6}$$

DLR Results

$f_0 = 135 \pm 1$ kHz

$C = 55.6 \pm 0.7$pF

We also verified that the driving frequency equaled the response frequency at resonance by looking at the FFT display, seen in Figure 10. Using the cursor function to measure where the highest peak was, we compared the frequencies of CH1 and CH2, and they were the same. One thing to note is that even at the lowest amplitude setting, a second harmonic remained where we should have obtained only one frequency peak (the leftmost, thin red peak is at 0 kHz and taken to be just a dummy marker, not a first harmonic). This may be due to the oscilloscope's limited low amplitude range. It also may be the cause of the nonlinearity observed in the low side tail of Figure 9.

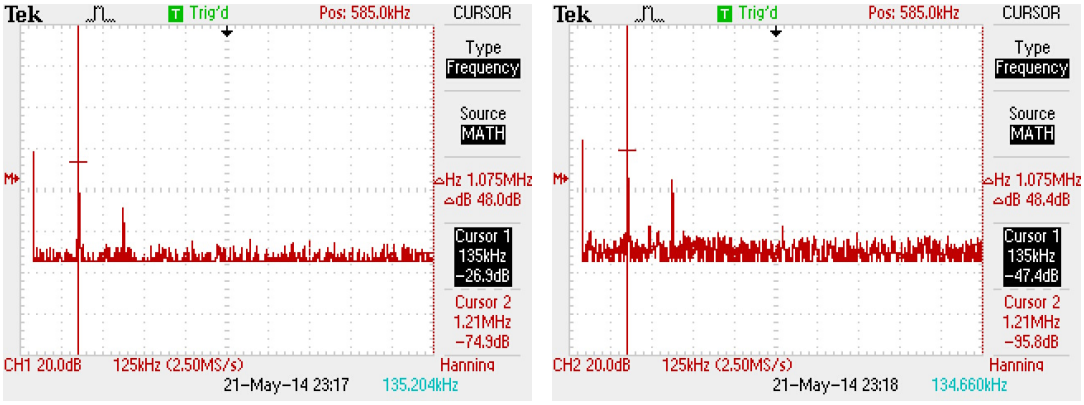

(a) (b)

Figure 10: The driving frequency (CH1, right) compared with the response frequency (CH2, left) of the DLR circuit at low amplitudes. Here, the highest peak is covered by the cursor line.

Turning off the attenuator and scanning through higher amplitudes generated very distinct responses in the FFT of the measured signal. As the driving voltage was increased, a threshold would be passed and suddenly many peaks in the FFT would appear. These were measured to be integer multiples of the resonance frequency (highest peak). From this we concluded that these are higher order harmonics of the circuit that become amplified at high amplitudes. We captured the FFT of four distinct regimes, characterized by the number of harmonics, in Figure 11. One thing to note is that we believe that the leftmost thin red "peak" in the pictures is not actually a harmonic, since it is at 0 kHz. It may actually be a dummy marker that the oscilloscope automatically generates.

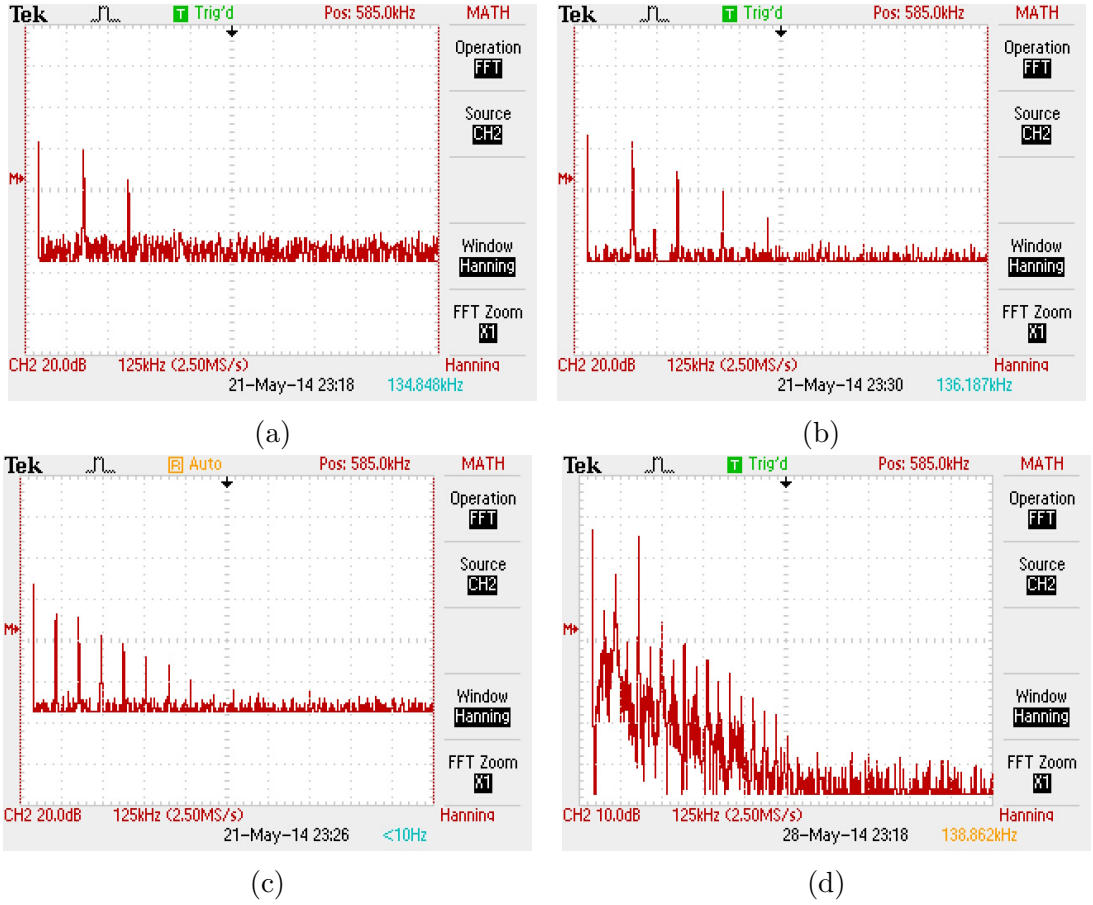

(a) (b)

(c) (d)

Figure 11: The four regions of interest in the DLR circuit: the linear region (a), the distortion region (b), the nonlinear region (c) and the chaotic region (d).

We also noticed that even at the lowest possible driving voltage with the attenuator activated, we could not remove all but one peak in the frequency spectrum, as in Figure 11 (a), where there are two harmonics visible. This may be due to a limited range of low amplitudes that the function generator can produce. Another possibility is that there are internal resonances within the function generator or the scope.

As we increased the driving voltage to near maximum, we compared the FFT with the normal voltage/time display and observed incredibly noisy signal and a continuous smearing of frequencies present in the circuit, as in Figures 11 (d) and 13. This signified that we were operating within the chaotic regime of the circuit.

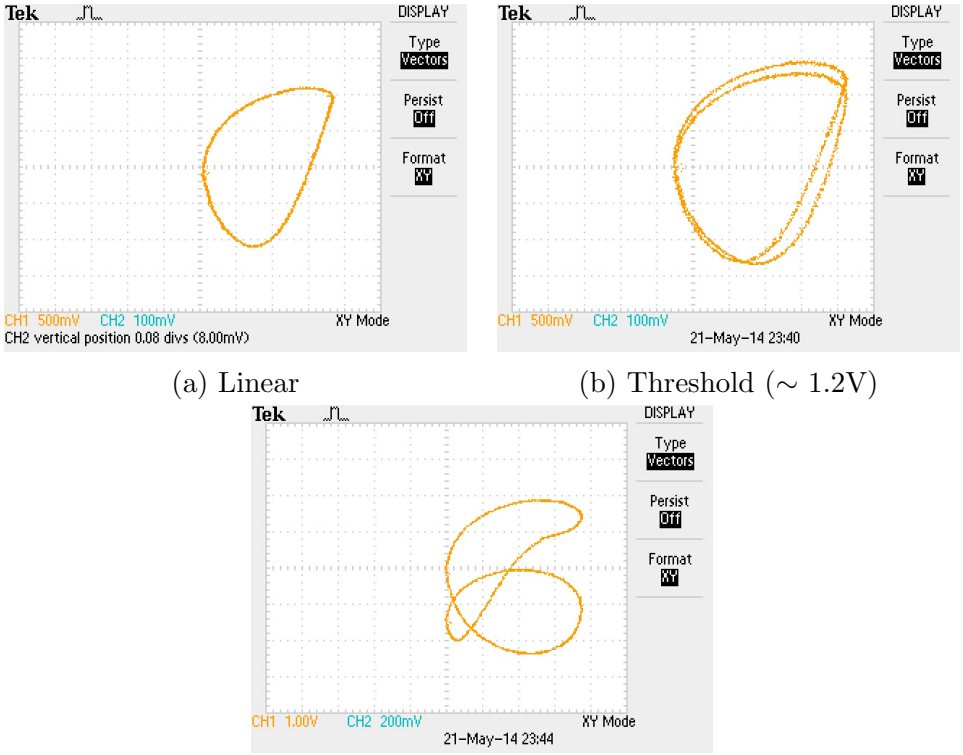

(a) Linear

(b) Threshold ($\sim$ 1.2V)

(c) Distortion

Figure 12: The XY display (IV curve) on the oscilloscope showing the bifurcation transition between the linear and distortion regions of the DLR circuit.

Figure 12 illustrates how the XY curve on the oscilloscope changes as we increased the input amplitude. The single loop can be thought of as an even trading-off of the current and voltage in the circuit. In other words, there is a constant phase between $I(t)$ and $V(t)$. As the loop splits, the current and voltage maintain a relatively constant phase between them, but they become centered about a slightly higher (or lower) range of current/voltage amplitudes. They also return to their origin in twice the time; this is the onset of period doubling. As the loops split dramatically as in figure 12 (c), period doubling remains but now the phase difference between the current and voltage is highly time dependent.

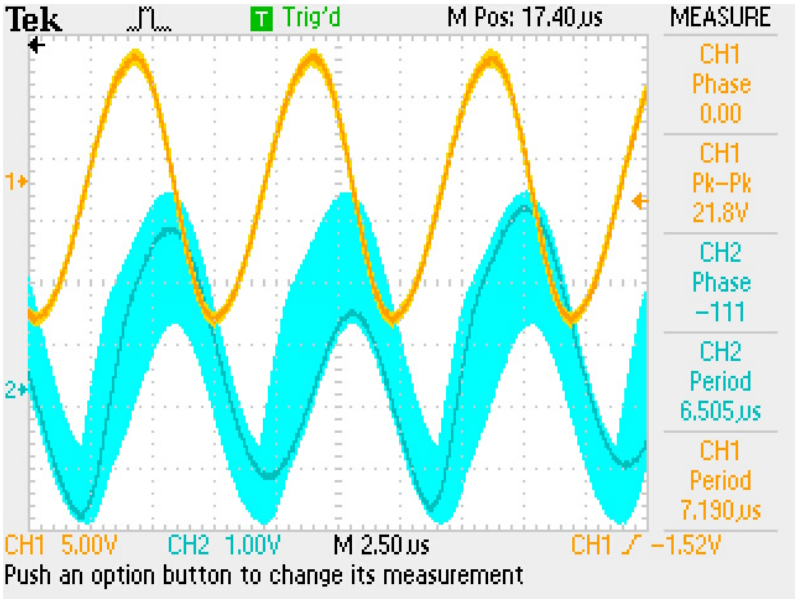

Figure 13: The chaotic regime signal voltage (blue) and input voltage (yellow) with infinite persistence.

Figure 13 shows the voltage/time graph for the DLR circuit in the chaotic regime. The persist function on the oscilloscope allowed us to see the range of amplitudes and phases of the signal, illustrating the indeterministic behavior. Although it could not be captured as a single picture, one can imagine the real time signal as a rapidly changing sine wave. It's behavior was so wild that we could not get the oscilloscope to trigger off of even the steadiest slope of the wave.

4 Summary

We obtained good results for the component values of the LRC and DLR circuits, as they matched up well with the claimed values. The only questionable result is that of the DLR circuit, which exhibited strange nonlinear behavior in the low-side tail of the frequency response. This may or may not have perturbed the value of the diode capacitance.

In all, many good observations were made of the two circuits, and the dynamical bridge between linearity, nonlinearity, and chaos, was illuminated.

5 Suggested Project: Chua's Circuit

We would like to suggest the possibility of going deeper into chaotic systems for future experimenters. As discussed in the introduction, Chua's circuit is a fine and doable example of a chaotic strange attractor circuit. There are some complications in its construction as a circuit, but it is well worth the investment of time and money for the educational opportunities it provides. In particular, it will be a unique and robust introduction to operational amplifiers for the undergraduate physics student.

Leon O. Chua invented Chua's circuit in 1983, and it has since been a "universal paradigm for chaos" [6]. Chua's circuit is shown in Figure 14. The capacitors C_1 and C_2 are normal capacitors, and the resistor R may be an active or precision resistor. The inductance L can be manifested through other means than a physical inductor; i.e., it may be constructed using a gyrator element instead of a normal coiled inductor. Since the inductance required to reproduce Chua's circuit is ideally very low in resistance ($\leq 30\Omega$), the gyrator may be preferable albeit more complicated to

create (see [3]).

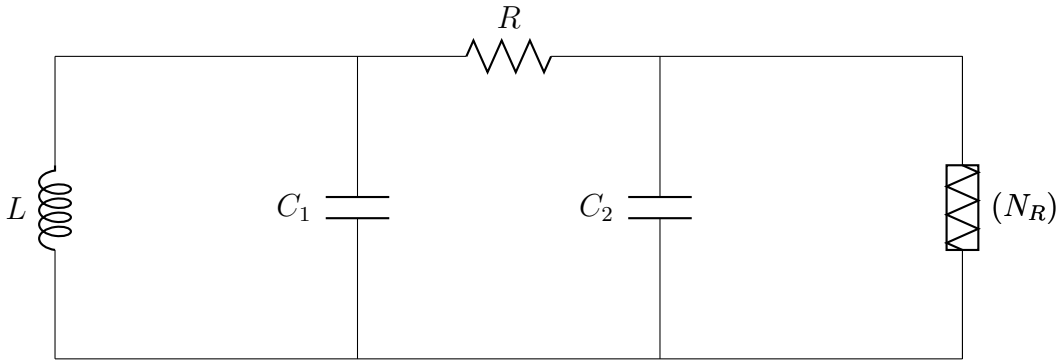

Figure 14: Chua's circuit diagram.

The feature of Chua's circuit is Chua's diode. Chua's diode is a type of nonlinear resistor, which can be realized in many ways and is best described using a system of linear equations. One possible realization of the diode is shown in Figure 16.

Chua's diode is described by the current across the diode, I_R as a function of the voltage across the diode V_R. It is a linear piecewise function:

$$I_R(V_R) = \begin{cases} G_b V_R + (G_b - G_a)E & \text{if} \quad V_r < -E \\ G_a V_R & \text{if} \quad -E \leq V_R \leq E \\ G_b V_R + (G_a - G_b) & \text{if} \quad V_R > E \end{cases}$$

Here, $-E$ and E are the breakpoints of the piecewise function and G_a, G_b are the slopes of the inner and outer linear regions. These properties are best visualized in Figure 16. All of the parameters must be determined experimentally, since they depend on the types of components used [7].

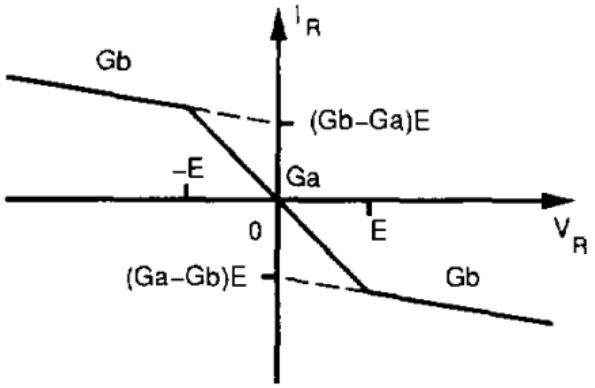

Figure 15: The IV diagram of Chua's diode.

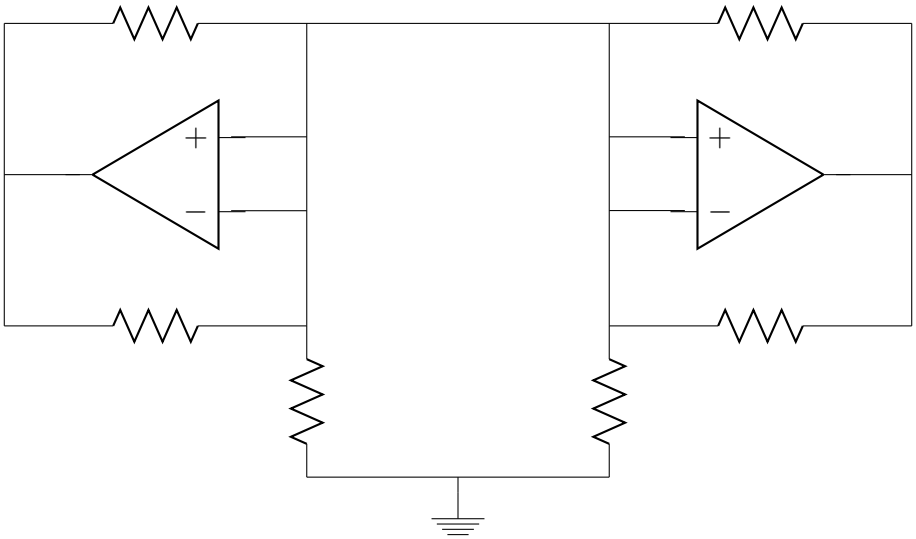

Figure 16: An op-amp realization of Chua's diode.

A very interesting phenomenon arises from Chua's circuit when driven; by projecting signals across three of the components onto a 3d display, the dynamics will produce a strange attractor. An attractor is a characteristic of a vector field that causes any trajectory in the field (it could be the trajectory of a moving particle or the time dependence of a current) to become "attracted" to a steady state of stable oscillations. An attractor becomes strange when the dynamics of trajectories about the attractor are chaotic. Visually, in a 3D space or even 2D space, attractors typically pull in trajectories into steady loops. In Chua's circuit, the strange attractor is known as a "double-scroll," because it has two possible steady states that trajectories join together like two scrolls. These shapes are shown in Figure 17.

In order to see the double scroll of Chua's circuit, one would need to plot the signals across both capacitors and the inductor in Figure 14.

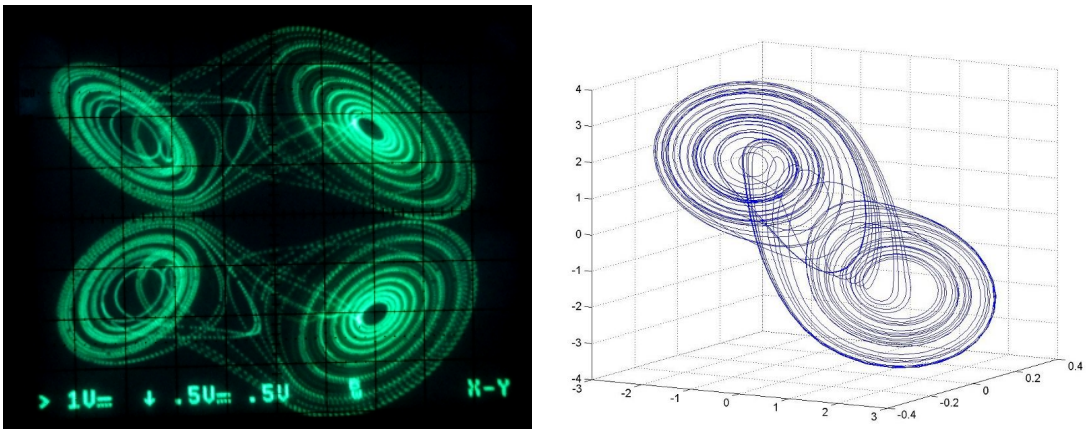

(a) (b)

Figure 17: The double-scroll strange attractor of Chua's circuit. (a) shows the attractor captured on an analog oscilloscope, while (b) shows the generation of the attractor in Matlab.

To recreate Chua's circuit, we suggest component values that follow those of [4]; $L = 18\text{mH}$, $C_1 = 100\text{nF}$, $C_2 = 10\text{nF}$, and $R = 1675\Omega$. To build the diode and to fully realize the double scroll behavior, we recommend following [3] for detailed and in depth tutorial.

6 Acknowledgments

I would like to thank Alice Durand and professor David Smith at UC Santa Cruz for all of their help and motivation during my sojourn into experimental physics. I also wish to thank professor Stefano Profumo for his insight into chaos that he shared with us in his Fall 2013 *Mechanics* lectures.

7 Appendix

References

[1] Strogatz, Steven H. *Nonlinear Dynamics and Chaos.* N.p.: Perseus , LLC, 1994. Print.

[2] Williams, Garnett P. *Chaos Theory Tamed.* Washington, D.C.: Joseph Henry, 1997. Print.

[3] Siderskiy, Valentin. "Components for Building Chua's Circuit." *Components for Building Chua's Circuit.* N.p., 2014. Web. http://www.chuacircuits.com/howtobuild2.php.

[4] Korneta, Wojcie, Iacyel Gomez, Claudio R. Mirasso, and Raúl Toral. "Phase-shifts in Stochastic Resonance in a Chua Circuit." (2008): n. pag. ArXiv. Web.

[5] Siderskiy, Valentin. "Matlab Simulation Code for Chua's Circuit." *Chua Circuits.* N.p., n.d. Web. http://www.chuacircuits.com/matlabsim.php.

[6] Chua, Leon O., Chai Wah Wu, Anshan Huang, and Guo-Qun Zhong. "A Universal Circuit for Studying and Generating Chaos - Part I: Routes to Chaos." IEEE 40.10 (1993): n. pag. Http://www.eecs.berkeley.edu/. Web.

[7] Kennedy, Michael P. "Three Steps to Chaos-Part 11: A Chua's Circuit Primer." *IEEE TRANSACTIONS ON CIRCUITS AND SYSTEMS- I : FUNDAMENTAL THEORY AND APPLICATIONS* 40.10 (1993): n. pag. EECS Instructional Support. Web.